

Accepted Manuscript

(*E*)-3-Heteroarylidenechroman-4-ones as potent and selective monoamine oxidase-B inhibitors

Nicoletta Desideri, Luca Proietti Monaco, Rossella Fioravanti, Mariangela Biava, Matilde Yáñez, Stefano Alcaro, Francesco Ortuso



PII: S0223-5234(16)30264-1

DOI: [10.1016/j.ejmech.2016.03.081](https://doi.org/10.1016/j.ejmech.2016.03.081)

Reference: EJMECH 8506

To appear in: *European Journal of Medicinal Chemistry*

Received Date: 5 August 2015

Revised Date: 23 March 2016

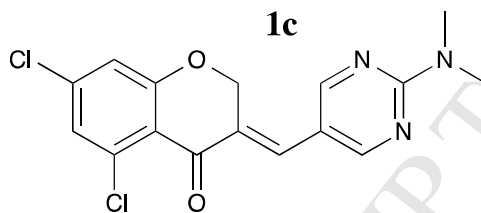
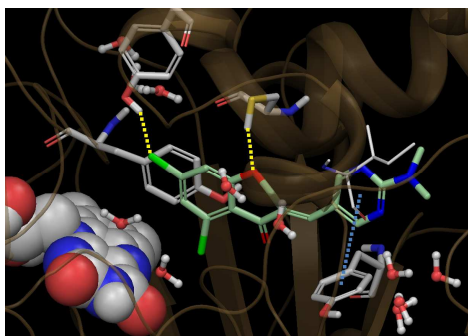
Accepted Date: 26 March 2016

Please cite this article as: N. Desideri, L. Proietti Monaco, R. Fioravanti, M. Biava, M. Yáñez, S. Alcaro, F. Ortuso, (*E*)-3-Heteroarylidenechroman-4-ones as potent and selective monoamine oxidase-B inhibitors, *European Journal of Medicinal Chemistry* (2016), doi: 10.1016/j.ejmech.2016.03.081.

This is a PDF file of an unedited manuscript that has been accepted for publication. As a service to our customers we are providing this early version of the manuscript. The manuscript will undergo copyediting, typesetting, and review of the resulting proof before it is published in its final form. Please note that during the production process errors may be discovered which could affect the content, and all legal disclaimers that apply to the journal pertain.

(E)-3-Heteroarylidenechroman-4-ones as potent and selective monoamine oxidase-B inhibitors

Nicoletta Desideri, Luca Proietti Monaco, Rossella Fioravanti, Mariangela Biava, Matilde Yáñez, Stefano Alcaro, Francesco Ortuso.



hMAO-B IC_{50} =10.58 nM, SI > 9452

(*E*)-3-Heteroarylidenechroman-4-ones as potent and selective monoamine oxidase-B inhibitors

Nicoletta Desideri ^{a,*}, Luca Proietti Monaco ^a, Rossella Fioravanti ^a, Mariangela Biava ^a, Matilde Yáñez ^b, Stefano Alcaro ^c, Francesco Ortuso ^c.

^aDipartimento di Chimica e Tecnologie del Farmaco, Sapienza - Università di Roma, P.le Aldo Moro, 5, 00185 Rome, Italy

^b Departamento de Farmacología, Facultad de Farmacia, Universidad de Santiago de Compostela, Campus Universitario Sur, E-15782 Santiago de Compostela (La Coruña), Spain

^cDipartimento di Scienze della Salute, Università “Magna Græcia” di Catanzaro, Campus Universitario “S. Venuta”, Viale Europa, 88100, Catanzaro, Italy.

* To whom correspondence should be addressed. Phone: +39-06-49913892. E-mail: nicoletta.desideri@uniroma1.it

Abstract – A series of (*E*)-3-heteroarylidenechroman-4-ones (**1a-r**) was designed, synthesized and investigated *in vitro* for their ability to inhibit the enzymatic activity of both human monoamine oxidase (hMAO) isoforms, hMAO-A and hMAO-B. All the compounds were found to be selective hMAO-B inhibitors showing IC₅₀ values in the nanomolar or micromolar range. (*E*)-5,7-Dichloro-3-[[2-(dimethylamino)pyrimidin-5-yl]methylene]chroman-4-one (**1c**) was the most interesting compound identified in this study, endowed with higher hMAO-B potency (IC₅₀ = 10.58 nM) and selectivity (SI > 9452) with respect to the reference selective inhibitor selegiline (IC₅₀ = 19.60 nM, IC₅₀ > 3431). Molecular modeling studies were performed for rationalizing at molecular level the target selective inhibition of our compounds, revealing a remarkable contribution of hydrogen bond network and water solvent.

Keywords: Monoamine oxidases; Selective hMAO-B inhibitors; Chroman-4-ones; Homoisoflavonoids; Docking studies

1. Introduction

Monoamine oxidases (MAOs) are flavin-containing enzymes that catalyze the oxidative deamination of a variety of monoamines including neurotransmitters such as serotonin, norepinephrine, epinephrine and dopamine, as well as dietary amines. Two different isoforms have been identified, MAO-A and MAO-B, both associated with the outer membrane of mitochondria. The two isoenzymes are encoded by separate genes and show different tissue distribution, and distinct substrate and inhibitor specificities. MAO-A preferentially catalyzes the oxidative deamination of neurotransmitters, serotonin, norepinephrine and epinephrine and it is selectively inhibited by clorgyline and moclobemide, irreversible and reversible inhibitor, respectively. MAO-B preferentially metabolizes β -phenethylamine and benzylamine and it is selectively and irreversibly inhibited by selegiline. Tyramine, tryptamine and dopamine, are substrates for both isoforms [1]. MAO-A inhibitors are indicated for the treatment of psychiatric disorders, while MAO-B inhibitors are used in the therapy of Parkinson's disease and have been proposed for the treatment of Alzheimer's disease [2-4].

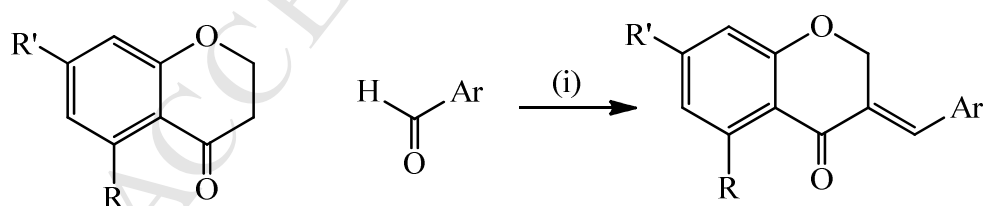
The MAO inhibitory activities of several classes of synthetic flavonoids were previously investigated [5-10]. In particular, we reported the potent and selective hMAO-B inhibitory properties of synthetic (*E*)-3-benzylidenechroman-4-ones, structurally related to natural homoisoflavonoids [7]. With the aim to further explore the structure-activity relationships of this new class of MAO-B inhibitors, we planned the replacement of the 3-benzylidene moiety with a variety of heteroarylidene substituents, including either five-membered or six-membered heterocycles. Therefore, a series of (*E*)-3-heteroarylidenechroman-4-ones **1a-r** was synthesized and evaluated in vitro for their ability to inhibit the enzymatic activity of both hMAO isoforms.

2. Results and discussion

2.1 Chemistry

The most common synthetic procedure to obtain (*E*)-3-benzylidenechroman-4-ones involves acid or base catalyzed condensation of chroman-4-ones with the appropriate benzaldehyde [11]. The corresponding *Z*-isomers were usually obtained by photoisomerization of the synthesized *E*-isomers [12-15]. The ¹HNMR spectra allow the unambiguous assignment of *E* and *Z* configurations to these stereoisomers. In particular, the signal of the olefinic proton in the *E* isomers appears at about 7.7 ppm, due to the effect of the near carbonyl group, and the signal of C-2 protons was measured at about 5.3 ppm, owing to the proximity with the phenyl ring. Both signals were considerable upfield shifted for the *Z*-isomers that show the signals at about 6.8 ppm and 4.9 ppm, respectively [12-15].

With similar synthetic procedures, several (*E*)-3-heteroarylidenechroman-4-ones were synthesized starting from chroman-4-ones and different heteroaryl aldehydes [13,16-20]. As illustrated in Scheme 1, we conveniently obtained the designed (*E*)-3-heteroarylidenechroman-4-ones **1a-r** using pyrrolidine as catalyst of the condensation. All the synthesized compounds were obtained as a single stereoisomer and the ¹HNMR spectra allow the assignment of the *E* configuration to the exocyclic double bond on the basis of the chemical shifts of the olefinic proton (ranging from 7.59 ppm to 8.11 ppm) and of the C-2 methylene protons (ranging from 5.29 ppm to 5.85 ppm).



Scheme 1. Reagents and conditions: (i) Pyrrolidine, dry MeOH: r.t., 1-24h (**1a-e** and **1h-r**) or 120 °C, 1h (**1f** and **1g**).

2.2 Biochemistry

The effects of the tested compounds on hMAO-A and hMAO-B enzymatic activities were evaluated by measuring the inhibition of the production of hydrogen peroxide from *p*-tyramine, using

the Amplex Red MAO assay kit and microsomal MAO isoforms prepared from insect cells (BTI-TN-5B1-4) infected with recombinant baculovirus containing cDNA inserts for hMAO-A or hMAO-B. The hMAO activity was evaluated by measuring the fluorescence generated by resorufin following the general procedure previously described by us [21]. In our experiments, hMAO-A displayed a Michaelis constant (K_M) of $514 \pm 46.8 \mu\text{M}$ and a maximum reaction velocity (V_{max}) of $301.4 \pm 27.9 \text{ nM/min/mg}$ protein, whereas hMAO-B showed a K_M of $104.7 \pm 16.3 \mu\text{M}$ and a V_{max} of $28.9 \pm 6.3 \text{ nM/min/mg}$ protein ($n = 5$).

The hMAO inhibition data and the hMAO-B selectivity indexes ($\text{SI} = \text{IC}_{50} \text{ MAO-A} / \text{IC}_{50} \text{ MAO-B}$) obtained for the (*E*)-3-arylidenechroman-4-ones **1a-r** and for the reference inhibitors (**clorgyline**, **selegiline**, **iproniazid**, **moclobemide** and **isatin**) are reported in Table 1. The new tested compounds inhibited the hMAO-B enzymatic activity in the micromolar or submicromolar range, conversely, no inhibition or poor efficacy was observed against hMAO-A, up to the highest concentration tested ($100 \mu\text{M}$).

In the series of (*E*)-3-heteroarylidenechroman-4-ones containing a five-membered heterocycle (**1l-r**), the thiophene substituted analogues (**1q** and **1r**) were the most potent and selective inhibitors of hMAO-B activity ($\text{IC}_{50} = 1.13 \mu\text{M}$ and $1.73 \mu\text{M}$, $\text{SI} = 88$ and 58 , respectively), whereas the furan-2-yl derivative (**1p**) ($\text{IC}_{50} = 3.77 \mu\text{M}$, $\text{SI} = 27$) was about 3-fold less potent and selective than the corresponding thiophen-2-yl analogue (**1q**) ($\text{IC}_{50} = 1.13 \mu\text{M}$, $\text{SI} = 88$). A further reduction in potency and selectivity was observed for compounds containing a pyrrole (**1l**) or an imidazole ring (**1m-o**). A comparison of the potency of the three imidazol-4-yl derivatives (**1m-o**) revealed that either the introduction of a methoxy group at position 7 (**1o**) or two chlorine atoms at the positions 5 and 7 (**1n**) of the chromanone ring, led to hMAO-B inhibitors about 2-fold more potent and selective than the unsubstituted analogue **1m**.

However, the replacement of the 3-benzylidene substituent with a five-membered heteroarylidene moiety generally led to a reduction in potency toward hMAO-B with respect to previously tested (*E*)-3-

benzylidenechroman-4-ones [7]. Conversely, highly potent and selective hMAO-B inhibitors were obtained with the introduction of a six-membered heterocycle or a bulkier indole ring. (*E*)-5,7-Dichloro-3-[[2-(dimethylamino)pyrimidin-5-yl]methylene]chroman-4-one (**1c**) was the most potent and selective compound ($IC_{50} = 10.58$ nM, $SI > 9452$) within the entire series of inhibitors, showing hMAO-B potency and selectivity even better than the reference selective MAO-B inhibitor selegiline ($IC_{50} = 19.60$ nM, $SI = 3431$).

It is worth noting that, either the presence of two chlorine atoms at the positions 5 and 7 of the chroman-4-one ring or the 2-dimethylamino group on the pyrimidine ring are necessary for the potent hMAO-B inhibitory activity. In fact, the substitution with a methoxy group at position 5 of the chroman-4-one ring (**1d**) produced a dramatic loss of hMAO-B potency and selectivity ($IC_{50} = 10.40$ μ M, $SI > 9.6$) whereas the removal of both the chlorine substituents resulted in compound **1b**, about 22-fold less potent and selective ($IC_{50} = 241.11$ nM, $SI > 415$) than **1c**. Moreover, the replacement of the dimethylamino group with the amino one provided a 75-fold less active and selective compound (**1a**) ($IC_{50} = 18.33$ μ M, $SI > 5.5$) with respect to **1b**. A similar behaviour was also observed for the (*E*)-3-benzylidenechroman-4-ones previously tested [7].

Among the pyridine substituted derivatives (**1e-j**), only the 3-[[6-(dimethylamino)pyridin-3-yl]methylene] analogue (**1i**) showed activity in the submicromolar range ($IC_{50} = 213.22$ nM, $SI > 469$). This compound exhibited hMAO-B potency and selectivity comparable to the corresponding pyrimidinyl derivative (**1b**) ($IC_{50} = 241.11$ nM, $SI > 415$). Surprisingly, the introduction of chlorine atoms at positions 5 and 7 of the chromone ring (**1j**) produced a marked reduction in potency and selectivity when compared to **1i**.

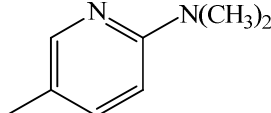
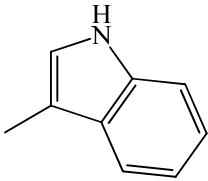
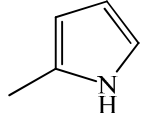
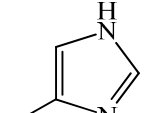
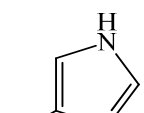
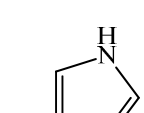
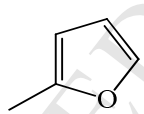
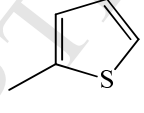
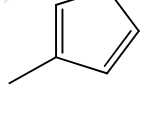
Finally, the substitution with a bulkier indole ring resulted in compound **1k**, exhibiting submicromolar potency and high selectivity toward hMAO-B ($IC_{50} = 181.45$ nM, $SI = 551$).

To investigate whether the most potent hMAO-B inhibitor (**1c**) is a reversible or irreversible enzyme inhibitor, an effective dilution method was used [22]. Following this method, reversible inhibitors show a linear progress with a slope equal to about 91% of the slope of the control sample,

while irreversible inhibitors reach only about 9% of this slope. The results obtained for the tested compound (**1c**), for the reversible inhibitor isatin and for the irreversible inhibitor selegiline are presented in Figure 1. The data suggest that **1c** is a partially reversible inhibitor. In fact, only a modest recovery of MAO-B activity was observed after dilution of samples previously incubated with this compound.

Table 1. IC_{50} and SI values for the inhibitory effects of (*E*)-3-heteroarylidenochroman-4-ones **1a-r** and reference inhibitors on the enzymatic activity of human recombinant MAO isoforms expressed in baculovirus infected BTI insect cells.

Comp	R	R ₁	Ar	hMAO-A (IC_{50}) (μ M)	hMAO-B (IC_{50}) (μ M)	SI ^b
1a	H	H		**	18.33 \pm 1.76	> 5.5
1b	H	H		**	241.11 $\times 10^{-3} \pm$ 14.18 $\times 10^{-3}$	> 415
1c	Cl	Cl		**	10.58 $\times 10^{-3} \pm$ 1.25 $\times 10^{-3}$	> 9452
1d	H	OCH ₃		**	10.40 \pm 1.28	> 9.6
1e	H	H		**	2.94 \pm 0.17	> 34
1f	H	H		**	12.44 \pm 0.67	> 8
1g	H	H		**	8.23 \pm 0.22	> 12
1h	H	H		**	2.39 \pm 0.21	> 42
1i	H	H		**	213.22 $\times 10^{-3} \pm$ 24.43 $\times 10^{-3}$	> 469

1j	Cl	Cl		***	10.51 ± 1.87	9.5 [#]
1k	H	H		***	181.45 × 10 ⁻³ ± 8.60 × 10 ⁻³	551 [#]
1l	H	H		***	13.76 ± 0.57	7.3 [#]
1m	H	H		***	20.20 ± 0.12	5 [#]
1n	Cl	Cl		***	10.21 ± 1.36	9.8 [#]
1o	H	OCH ₃		***	10.62 ± 0.71	9.4 [#]
1p	H	H		***	3.77 ± 0.35	27 [#]
1q	H	H		***	1.13 ± 0.24	88 [#]
1r	H	H		***	1.73 ± 0.12	58 [#]
Clorgyline				4.46 × 10 ⁻³ ± 0.32 × 10 ⁻³ ^a	61.35 ± 1.13	0.000073
Selegiline				67.25 ± 1.02 ^a	19.60 × 10 ⁻³ ± 0.86 × 10 ⁻³	3431
Iproniazid				6.56 ± 0.76	7.54 ± 0.36	0.87
Moclobemide				361 ± 19.37	*	< 0.36
Isatin				**	34.39 ± 1.73	> 3

All IC₅₀ values shown in this table are the mean ± S.E.M. from five experiments. Level of statistical significance: ^aP < 0.01 versus the corresponding IC₅₀ values obtained against MAO-B, as determined by ANOVA/Dunnett's. ^b SI: hMAO-B selectivity index = IC₅₀ (hMAO-A)/IC₅₀ (hMAO-B). * Inactive at 1 mM (highest concentration tested). ** Inactive at 100 μM (highest concentration tested).*** 100 μM inhibits the corresponding MAO activity by approximately 40-50%. At

higher concentration the compounds precipitate. # Values obtained under the assumption that the corresponding IC_{50} against MAO-B is the highest concentration tested (100 μ M).

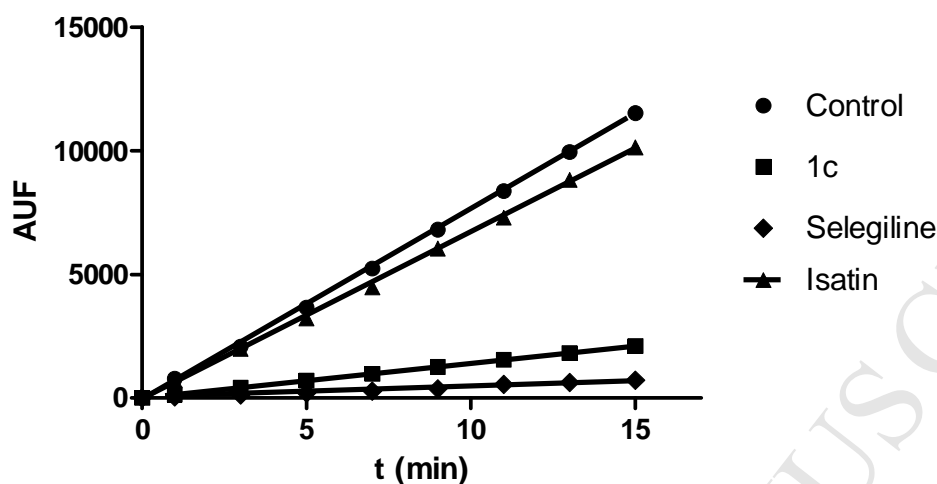


Figure 1. Recovery of hMAO-B enzymatic activity after dilution and following incubation (30 min at room temperature) of the 100x-enzyme concentration with 10-fold IC_{50} concentration of compound **1c**, isatin or selegiline. The control was carried out by pre-incubating in the absence of inhibitor and diluting in the same way.

2.3 Docking studies

To rationalize at molecular level the inhibition of hMAOs by the compounds, molecular modelling studies were carried out. The binding capabilities of **1a-r** were investigated, with respect to hMAO-A and hMAO-B receptor models, by means of docking simulation (Experimental section). All compounds recognized both isozymes active sites. The hMAO-B was the preferred target but none of theoretical scoring functions, available in Glide software, was in accord to experimental IC_{50} data (Table S1). Generally, even if head-tail configurations were observed, the binding modes of our molecules reported the chroman-4-one moiety located towards the FAD cofactor establishing pi-pi stacking to hMAO-A Tyr407 and/or Tyr444 and the corresponding hMAO-B Tyr398 and/or Tyr435. The Ar substituent was positioned at the active site entrance area in well known hydrophobic regions suggesting possible T-shape stacking contacts to the sidechain of hMAO-A Phe208 and hMAO-B Tyr407. According to literature data [23], the hydrophobic area in hMAO-B is larger than in hMAO-A and could

better accommodate Ar substituent of our compounds resulting in a superior stabilisation of the related complexes. The graphical analysis of the docking results showed a hydrogen bond between the hMAO-B Cys172 sidechain and the chroman-4-one common moiety of all ligands, except **1b** that reported a head-tail recognition with respect to **1c**. In details, the previous interaction involved the sp³ oxygen atom of **1c**, **1d**, **1f**, **1j**, **1m** and **1n**, whereas, due to different binding modes, **1e**, **1g-i**, **1k-l**, **1o-r** established hydrogen bond to Cys172 sidechain by means of their sp² chroman-4-one oxygen atom. The equivalent residue in hMAO-A is Asn181 but its sidechain was involved in hydrogen bond to Phe177 backbone preventing interaction with the compounds. Taking into account the better accommodation and hydrogen bond contribution in hMAO-B, the chroman-4-one and the Ar substituent could be considered as the key moieties of the compounds to exert affinity and selectivity to MAOs. However, the poor agreement among theoretical and experimental data prompted us to improve our study including the water solvent effects to the ligand target recognition. As a consequence, the most stable complex models of **1c** into the hMAO-A and hMAO-B were explicitly solvated and submitted to molecular dynamics (MD) simulation (Experimental section). Both MD starting structures revealed water molecules into the active site engaging hydrogen bonds to target residues such as hMAO-A Gly110, Ile207, Phe208, Ser209, Thr211 and Gly214 and hMAO-B Pro102, Thr201, Cys172, Ile198 and Tyr435. Notably, in both complexes, one solvent molecule was interacting with **1c** reporting hydrogen bond to chroman-4-one sp² oxygen or to pyrimidine nitrogen in hMAO-A and hMAO-B respectively. For a deeper investigation on both the role of solvent and the induced fit phenomena, we submitted also the inhibitor free receptor models to the same MD protocol previously reported for the complexes (Experimental section). Interestingly, the mere MD starting structures revealed a protein desolvation penalty for the **1c** hMAO-A recognition with respect to the hMAO-B. In fact, in order to be accommodated into the active site, the inhibitor displaced 15 water molecules in the former case while in the second one 9 only (Figure S1).

Our study pursued by investigating the enzymes structural modification induced by **1c**. In fact, if a ligand binding generates strong perturbation of the target conformational properties, the recognition

could be energy penalized or prevented. In order to evaluate the **1c** influence in target stability, all MD trajectory frames were aligned to the corresponding enzyme starting structure and the root mean square deviation (RMSd) of the target not hydrogen atoms was computed (Figure 2).

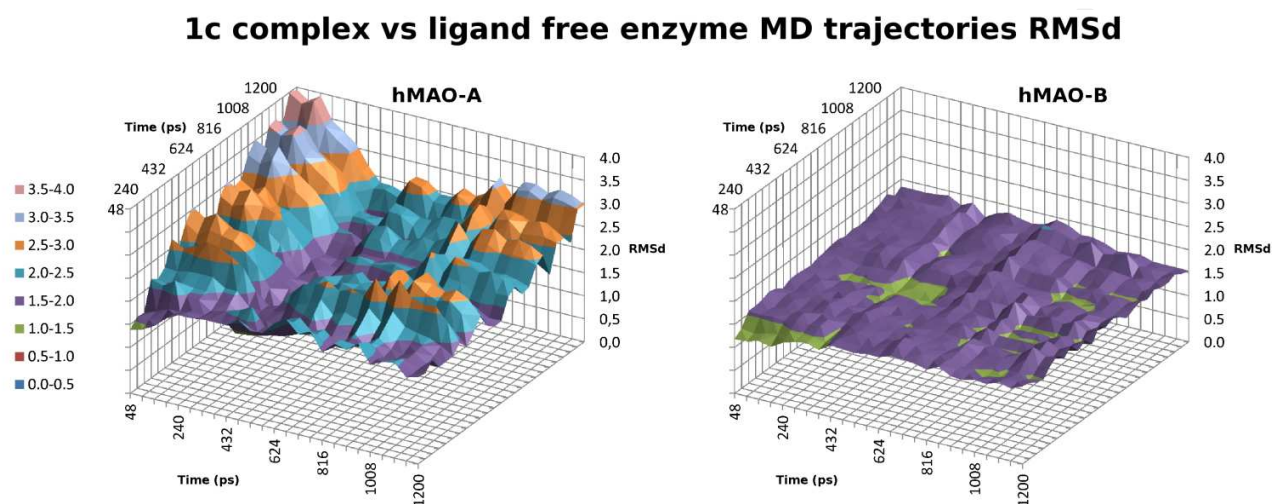


Figure 2. Root mean square deviation (in Å) of **1c** bound and ligand free hMAO-A and hMAO-B MD trajectories.

The RMSd data remarked significant enzyme isoform dependent differences. Actually, the ligand induced a perturbation of the hMAO-A stronger than hMAO-B as reported by RMSd values wider in the former case with respect to the second one. Furthermore, the MD single trajectories RMSd analysis revealed that **1c** stabilized the hMAO-B conformers close to the starting structure while in hMAO-A the ligand influence was completely opposite. (Figure S2)

After the above reported indication, MD trajectories of **1c** complexes were examined for highlighting other interactions useful to explain the experimentally observed hMAO selectivity. We focused our attention on **1c** targets stacking contacts, hydrogen and halogen bonds to both hMAOs and solvent molecules (Figure S3-S5). Stacking contacts, already reported by docking, were stable during MD. Our inhibitor spent 76% and 84% of the simulation time, in hMAO-A and hMAO-B respectively, establishing pi-pi interaction between its chroman-4-one moiety and the FAD close tyrosine residues while T-shape stacking contacts to hMAO-A Phe208 and hMAO-B Tyr407 sidechains, only suggested

by docking, were simultaneously observed in 16% and 8% of the simulation time, respectively (Figure S3). The stabilizing effect can be considered almost equivalent confirming our idea that stacking contacts are related to **1c** MAO affinity but have not a pivotal role in terms of enzyme isoform selectivity. The same considerations can be done after the halogen bond (HalB) network analysis that reported productive contribution of chlorine substituent and a solvent key role (Figure S4). In fact, chlorine moiety showed a similar HalB frequency in both targets (52% in hMAO-A and 48% in hMAO-B) but in the enzyme isoform B the productive interaction was often mediated by water molecules. Conversely, hydrogen bond (HB), involving the target both directly or by means of water bridges, should be considered the driving force of **1c** MAO discrimination. Actually, our ligand established HB to hMAO-B for a MD simulation time significantly longer in hMAO-B (80%) than in hMAO-A (52%) and in the former case the 32% double HBs, one target directed and one water mediated, were observed (Figure S5).

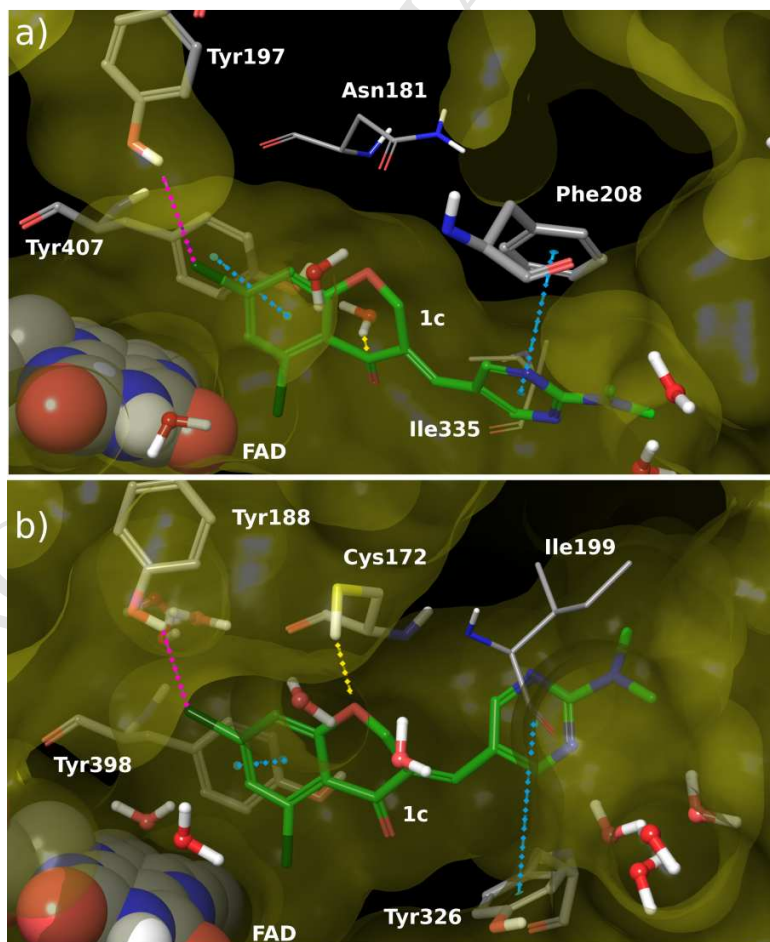


Figure 3. Representative binding modes of **1c** into the a) hMAO-A and b) hMAO-B. The inhibitor is reported in green carbon polytube. Relevant interacting residues are in CPK polytube. Enzyme isoform specific amino acids are depicted in CPK thin tube. FAD cofactor is showed in spacefill notation. Active site water molecules are represented in balls & sticks. The rest of the enzyme residues are illustrated as yellow transparent surface. Yellow, purple and blue dotted lines indicate hydrogen bond, halogen bond and stacking contacts respectively.

The reported interaction resulted in a similar orientation of **1c** in both targets (Figure 3). The graphical inspection of MD trajectories remarked the different shape of hMAO active sites. Actually, the mere replacement of hMAO-A Phe208 and Ile335 with the corresponding hMAO-B Ile199 and Tyr326 could be considered equivalent in terms of ligand interaction but such residue mutations opened in hMAO-B a large hydrophobic area that is not available in hMAO-A.

Comparing all molecular modelling results to experimental IC₅₀ data, it is possible to rationalize structure activity relationship of our inhibitors. Actually, halogen atoms or hydrogen bond acceptors can be suggested for the common scaffold R₁ substituent. Such moieties can productively interact to hMAO-A Tyr197 and hMAO-B Tyr188. In order to establish hydrogen bond to the solvent and pi-pi stacking and in both isozymes, the Ar group should be an aromatic heterocycle. Its steric hindrance can contribute to the selectivity, actually 5 member rings can easily fit in both isoform while amino or dimethylamino *p*-substituted 6 member rings or indole can be accommodate in hMAO-B better than in hMAO-A. Finally, as already reported [24], the replacement of hMAO-A Asn181 by the hMAO-B Cys172 plays a pivotal role in isoform selectivity.

3. Conclusions

We have designed, synthesized and investigated the hMAO inhibitory activity of a series of (*E*)-3-heteroarylidenechroman-4-ones, structurally related to homoisoflavonoids. All the compounds exhibited selectivity for the hMAO-B isoform with potency in the nanomolar or micromolar range. Generally, the introduction of a six-membered heterocycle or a bulkier indole ring led to highly potent and selective hMAO-B inhibitors. In particular, compound **1c** showed higher potency and selectivity than the reference inhibitor selegiline. In addition, compound **1c** was found to be a partially reversible inhibitor

of hMAO-B enzymatic activity. Docking experiments coupled to explicit solvent MD, rationalized the structure activity relationships of our inhibitors. Water solvent effect revealed a key role for understanding the molecular recognition of both hMAO isoforms. The hydrogen bond established by our ligand chroman-4-one moiety to Cys172 and the steric hindrance of Ar substituent can be considered the main responsible of hMAO-B selectivity.

4. Experimental section

4.1. Chemistry

Chemicals were generally purchased from Sigma-Aldrich and used without further purification. 2-Aminopyrimidine-5-carboxaldehyde, and 6-(dimethylamino)nicotinaldehyde were purchased from ChemBridge. Melting points were determined on a Stanford Research Systems OptiMelt (MPA-100) apparatus and are uncorrected. ^1H NMR and ^{13}C NMR spectra were recorded in CDCl_3 or DMSO-d_6 on a Bruker AM-400 spectrometer, using TMS as internal standard. IR spectra were recorded in KBr disks on an FT-IR PerkinElmer Spectrum 1000. The structures of the synthesized compounds were characterized by elemental analysis, IR, ^1H NMR and ^{13}C NMR spectroscopy. Thin-layer chromatography (TLC) with pre-coated Silica Gel F254 plates was routinely used for checking the reactions. Components were visualised by UV light. Analyses of the elements (C,H,N,S,Cl) were within $\pm 0.4\%$ of the theoretical values.

4.1.1. Synthesis of 6-aminopyridine-3-carboxaldehyde.

A 1M solution of diisobutylaluminum hydride (DIBAL) in hexane (10 mL) was added to a solution of 6-amino-5-cyanopyridine (10 mmol) in dry THF (50 mL) cooled at $0\text{ }^\circ\text{C}$. The ice-bath was removed, and additional 7.1 mL of a 1M solution of DIBAL in hexane were added in two successive portions. After stirring for additional 30 min, the reaction was quenched by the dropwise addition of dry MeOH (15 mL). The mixture was partitioned between 100 mL of AcOEt and 70 mL of 2N HCl. The aqueous layer was treated with 75 mL of 2N NaOH and extracted with AcOEt. The organic layers were

washed with brine, dried over anhydrous Na_2SO_4 , filtered and evaporated to dryness. The residue was purified by column chromatography on silica gel eluting with $\text{CHCl}_3/\text{AcOEt}$ 1:4. Yield: 30%, mp = 174-175 °C. IR (KBr): 3366, 3121, 1659 cm^{-1} . ^1H NMR (CD_3OD , 400 MHz): δ (ppm) 9.67 (s, 1H, CHO), 8.41 (d, 1H, H2, $J_{2-4} = 1.6$ Hz), 7.87 (dd, 1H, H4, $J_{4-5} = 8.8$ Hz, $J_{2-4} = 1.6$ Hz), 6.63 (d, 1H, H5, $J_{4-5} = 8.8$ Hz), 3.31 (s, 2H, NH_2). ^{13}C NMR (CDCl_3 , 100 MHz): δ (ppm) 191.15, 164.46, 155.78, 137.39, 123.92, 109.99.

4.1.2. General procedure for the synthesis of (*E*)-3-heteroarylidenechroman-4-ones (**1a-r**)

METHOD A: Pyrrolidine (10 mmol) was added to a mixture of the appropriate chroman-4-one (6.7 mmol) and heteroaryl aldehyde (10 mmol) in dry MeOH (15 mL for **1a**, **1b**, **1e**, **1h**, **1k-r** and 30 mL for **1c**, **1d**, **1i**, **1j**). The reaction mixture was stirred at room temperature for 1-24h (1h for **1f**, 3h for **1l-q**, 24h for **1a-c**, **1h-j**, **1n**, and **1o**). The mixture was diluted with ice-water, and the precipitate was filtered off and washed with water. The crude solid was purified by column chromatography on silica gel, eluting with a mixture of AcOEt and CHCl_3 (3:1) (**1a-g** and **1i-r**) or CHCl_3 (**1h**) and crystallized from n-hexane.

METHOD B: (synthesis of **1f** and **1g**) A mixture of chroman-4-one (6.7 mmol), the appropriate pyridinecarbaldehyde (10 mmol) and pyrrolidine (10 mmol) was heated at 120 °C under stirring for 1h. After cooling, the mixture was diluted with ice-water, and the precipitate was filtered off and washed with water. The crude solid was purified by column chromatography on silica gel, eluting with a mixture of AcOEt and CHCl_3 (3:1), and crystallized from n-hexane.

4.1.2.1. (*E*)-3-[(2-Aminopyrimidin-5-yl)methylene]chroman-4-one (**1a**). Yield: 97%, mp = 260-261 °C. IR (KBr): 3304, 3160, 1670 cm^{-1} . ^1H NMR (DMSO-d_6 , 400 MHz): δ (ppm) 8.43 (s, 2H, H2', H6'), 7.87 (d, 1H, H5, $J_{5-6} = 7.6$ Hz), 7.60-7.56 (m, 2H, =CH, H7), 7.34 (s, 2H, NH_2), 7.12 (t, 1H, H6, $J_{5-6} = J_{7.6} = 7.6$ Hz), 7.05 (d, 1H, H8, $J_{7-8} = 8.0$ Hz), 5.43 (s, 2H, H2). ^{13}C NMR (DMSO-d_6 , 100 MHz): δ (ppm)

180.43, 162.83, 160.43, 160.20, 135.88, 131.50, 127.67, 127.10, 121.78, 121.42, 117.18, 116.79, 67.57.

Anal. Calcd. for C₁₄H₁₁N₃O₂: C, 66.40; H, 4.38; N, 16.59. Found: C, 66.59; H, 4.29; N, 16.68.

4.1.2.2. (*E*)-3-[[2-(Dimethylamino)pyrimidin-5-yl]methylene]chroman-4-one (**1b**). Yield: 89%, mp = 194-195 °C. IR (KBr): 1662 cm⁻¹. ¹H NMR (CDCl₃, 400 MHz): δ (ppm) 8.34 (s, 2H, H2', H6'), 8.01 (ddd, 1H, H5, *J*₅₋₆ = 8.0 Hz, *J*₅₋₇ = 2.0 Hz, *J*₅₋₈ = 0.4 Hz), 7.64 (t, 1H, =CH, *J*_{all} = 2.0 Hz), 7.47 (ddd, 1H, H7, *J*₇₋₈ = 8.4 Hz, *J*₇₋₆ = 7.2 Hz, *J*₅₋₇ = 2.0 Hz), 7.06 (ddd, 1H, H6, *J*₅₋₆ = 8.0 Hz, *J*₇₋₆ = 7.2 Hz, *J*₆₋₈ = 1.2 Hz), 6.96 (ddd, 1H, H8, *J*₇₋₈ = 8.4 Hz, *J*₆₋₈ = 1.2 Hz, *J*₅₋₈ = 0.4 Hz), 5.34 (d, 2H, H2, *J*_{all} = 2.0 Hz), 3.26 (s, 6H, 2CH₃). ¹³C NMR (CDCl₃, 100 MHz): δ (ppm) 181.40, 161.19, 160.90, 159.27, 135.68, 131.70, 128.47, 127.91, 122.05, 121.94, 117.82, 116.34, 67.85, 37.22. Anal. Calcd. for C₁₆H₁₅N₃O₂: C, 68.31; H, 5.37; N, 14.94; O, 11.37. Found: C, 68.16; H, 5.36; N, 14.80.

4.1.2.3. (*E*)-5,7-Dichloro-3-[[2-(dimethylamino)pyrimidin-5-yl]methylene]chroman-4-one (**1c**). Yield: 69%, mp = 181-182 °C. IR (KBr): 1677 cm⁻¹. ¹H NMR (CDCl₃, 400 MHz): δ (ppm): 8.30 (s, 2H, H2', H6'), 7.65 (s, 1H, =CH), 7.11 (s, 1H, H8), 6.95 (s, 1H, H6), 5.28 (s, 2H, H2), 3.26 (s, 6H, 2CH₃), ¹³C (CDCl₃, 100 MHz): δ (ppm) 178.63, 162.65, 161.29, 159.31, 139.91, 136.12, 132.82, 127.92, 125.70, 118.88, 117.31, 116.11, 68.09, 37.24. Anal. Calcd. for C₁₆H₁₃Cl₂N₃O₂: C, 54.87; H, 3.74; Cl, 20.25; N, 12.00. Found: C, 54.99; H, 3.80; Cl, 20.15; N, 11.87.

4.1.2.4. (*E*)-3-[[2-(Dimethylamino)pyrimidin-5-yl]methylene]-7-methoxychroman-4-one (**1d**). Yield: 90%, mp = 186-187 °C. IR (KBr): 1669 cm⁻¹. ¹H NMR (CDCl₃, 400 MHz): δ (ppm) 8.32 (s, 2H, H2', H6'), 7.94 (d, 1H, H5, *J*₅₋₆ = 8.8 Hz), 7.61 (s, 1H, =CH), 7.94 (d, 1H, H6, *J*₅₋₆ = 8.8 Hz), 6.41 (s, 1H, H8), 5.33 (s, 2H, H2), 3.84 (s, 3H, OCH₃), 3.26 (s, 6H, 2CH₃). ¹³C NMR (CDCl₃, 100 MHz): δ (ppm) 180.18, 165.97, 162.85, 161.15, 159.12, 130.89, 129.67, 128.52, 116.46, 115.73, 110.41, 100.80, 68.43,

55.87, 37.20. Anal. Calcd. for C₁₇H₁₇N₃O₃: C, 65.58; H, 5.50; N, 13.50. Found: 65.41; H, 5.52; N, 13.47.

4.1.2.5. (*E*)-3-[(*Pyridin-2-yl*)methylene]chroman-4-one (**1e**) Yield: 77%, mp = 139-140 °C (lit. 142°C) [17]. IR (KBr): 1673 cm⁻¹. ¹H NMR (CDCl₃, 400 MHz): δ(ppm) 8.65 (d, 1H, H3', *J*_{3'-4'} = 8.0 Hz), 8.02 (dd, 1H, H5, *J*₅₋₆ = 8.0 Hz, *J*₅₋₇ = 1.6 Hz), 7.74 (dt, 1H, H7, *J*₇₋₆ = *J*₇₋₈ = 8.0 Hz, *J*₅₋₇ = 1.6 Hz), 7.71 (t, 1H, =CH, *J*_{all} = 2.0 Hz), 7.51-7.47 (m, 2H, H5', H6'), 7.26-7.23 (m, 1H, H4'), 7.05 (t, 1H, H6, *J*₅₋₆ = *J*₇₋₆ = 8.0 Hz), 6.99 (d, 1H, H8, *J*₇₋₈ = 8.0 Hz), 5.92 (d, 2H, H2, *J*_{all} = 2.4 Hz). ¹³C NMR (CDCl₃, 100 MHz): δ (ppm) 182.26, 161.72, 154.18, 149.66, 136.54, 135.94, 134.33, 133.27, 127.95, 127.84, 123.15, 121.83, 121.63, 118.07, 68.41. Anal. Calcd. for C₁₅H₁₁NO₂: C, 75.94; H, 4.67; N, 5.90. Found: C, 76.16; H, 4.69; N, 5.85.

4.1.2.6. (*E*)-3-[(*Pyridin-4-yl*)methylene]chroman-4-one (**1f**). Yield: 40%, mp = 132-133 °C. IR (KBr): 1676 cm⁻¹. ¹H NMR (DMSO-d₆, 400 MHz): δ (ppm) 8.72 (d, 2H, H3', H5', *J*_{2'-3'} = 6.0 Hz), 8.03 (dd, 1H, H5, *J*₅₋₆ = 8.0 Hz, *J*₅₋₇ = 1.6 Hz), 7.75 (s, 1H, =CH), 7.52 (dt, 1H, H7, *J*₇₋₈ = *J*₇₋₆ = 8.0 Hz, *J*₅₋₇ = 1.6 Hz), 7.19 (d, 2H, H2', H6', *J*_{2'-3'} = 6.0 Hz), 7.10 (t, 1H, H6, *J*₇₋₆ = *J*₅₋₆ = 8.0 Hz), 6.99 (d, 1H, H8, *J*₇₋₈ = 8.0 Hz), 5.29 (s, 2H, H2). ¹³C NMR (DMSO-d₆, 100 MHz): δ (ppm) 180.77, 160.74, 149.99, 140.92, 136.52, 133.99, 133.47, 127.26, 123.93, 122.07, 121.13, 117.96, 67.02. Anal. Calcd. for C₁₅H₁₁NO₂: C, 75.94; H, 4.67; N, 5.90. Found: C, 75.81; H, 4.75; N, 5.93.

4.1.2.7. (*E*)-3-[(*Pyridin-3-yl*)methylene]chroman-4-one (**1g**) Yield: 61%, mp = 120-122 °C. IR (KBr): 1671 cm⁻¹. ¹H NMR (CDCl₃, 400 MHz): δ(ppm) 8.65 (dd, 1H, H4', *J*_{4'-5'} = 4.8 Hz, *J*_{2'-4'} = 1.2 Hz), 8.59 (d, 1H, H2', *J*_{2'-4'} = 1.2 Hz), 8.02 (dd, 1H, H5, *J*₅₋₆ = 7.6 Hz, *J*₅₋₇ = 1.6 Hz), 7.82 (s, 1H, =CH), 7.66 (d, 1H, H6', *J*_{6'-5'} = 7.6 Hz), 7.51 (ddd, 1H, H7, *J*₇₋₈ = 8.4 Hz, *J*₇₋₆ = 7.6 Hz, *J*₅₋₇ = 1.6 Hz), 7.41 (dd, 1H, H5', *J*_{6'-5'} = 7.6 Hz, *J*_{4'-5'} = 4.8 Hz), 7.09 (t, 1H, H6, *J*₅₋₆ = *J*₇₋₆ = 7.6 Hz), 6.98 (d, 1H, H8, *J*₇₋₈ = 8.4 Hz),

5.32 (d, 2H, H₂, $J_{\text{all}} = 2.0$ Hz). ¹³C NMR (CDCl₃, 100 MHz): δ (ppm) 181.60, 161.15, 150.22, 149.91, 137.04, 136.21, 133.23, 133.06, 130.43, 128.02, 123.62, 122.17, 121.79, 118.03, 67.28. Anal. Calcd. for C₁₅H₁₁NO₂: C, 75.94; H, 4.67; N, 5.90. Found: C, 75.78; H, 4.66; N, 5.89.

4.1.2.8. (*E*)-3-[(6-Aminopyrimidin-3-yl)methylene]chroman-4-one (**1h**). Yield: 84%, mp = 186-187 °C. IR (KBr): 3387, 3117, 1657 cm⁻¹. ¹H NMR (DMSO-d₆, 400 MHz): δ (ppm) 8.11 (s, 1H, =CH), 7.86 (d, 1H, H₅, $J_{5-6} = 8.0$ Hz), 7.59-7.53 (m, 3H, H_{2'}, H_{6'}, H₇), 7.11 (t, 1H, H₆, $J_{5-6} = J_{7.6} = 7.2$ Hz), 7.04 (d, 1H, H₈, $J_{7-8} = 8.4$ Hz), 6.69 (s, 2H, NH₂), 6.53 (d, 1H, H_{5'}, $J_{5'-6'} = 8.4$ Hz), 5.43 (s, 2H, H₂). ¹³C NMR (DMSO-d₆, 100 MHz): δ (ppm) 180.52, 160.32, 160.27, 152.40, 138.60, 135.63, 134.72, 127.04, 126.11, 121.69, 121.63, 118.19, 117.63, 107.73, 67.64. Anal. Calcd. for C₁₅H₁₂N₂O₂: C, 71.42; H, 4.79; N, 11.10. Found: C, 71.52; H, 4.83; N, 11.07.

4.1.2.9. (*E*)-3-[[6-(Dimethylamino)pyridin-3-yl]methylene]chroman-4-one (**1i**). Yield: 96%, mp = 160-162 °C. IR (KBr): 1655 cm⁻¹. ¹H NMR (CDCl₃, 400 MHz): δ (ppm) 8.19 (d, 1H, H_{2'}, $J_{2'-6'} = 2.4$ Hz), 8.00 (dd, 1H, H₅, $J_{5-6} = 7.6$ Hz, $J_{5-7} = 1.6$ Hz), 7.74 (s, 1H, =CH), 7.47-7.42 (m, 2H, H_{6'}, H₇), 7.05 (t, 1H, H₆, $J_{5-6} = J_{7-6} = 7.6$ Hz), 6.99 (d, 1H, H₈, $J_{7-8} = 8.0$ Hz), 6.56 (d, 1H, H_{5'}, $J_{5'-6'} = 9.2$ Hz), 5.38 (d, 2H, H₂, $J_{\text{all}} = 1.6$ Hz), 3.15 (s, 6H, 2CH₃). ¹³C NMR (CDCl₃, 100 MHz): δ (ppm) 181.73, 160.87, 158.93, 151.35, 138.73, 135.43, 135.14, 127.84, 127.23, 122.25, 121.77, 118.36, 117.73, 105.47, 68.04, 38.02. Anal. Calcd. for C₁₇H₁₆N₂O₂: C, 72.84; H, 5.75; N, 9.99. Found: C, 72.97; H, 5.77; N, 9.93.

4.1.2.10. (*E*)-5,7-Dichloro-3-[(6-(dimethylamino)pyridin-3-yl)methylene]chroman-4-one (**1j**). Yield: 11%, mp = 239-240 °C. IR (KBr): 1668 cm⁻¹. ¹H NMR (CDCl₃, 400 MHz): δ (ppm) 8.01 (s, 1H, =CH), 7.30 (s, 1H, H_{2'}), 7.24 (d, 1H, H_{6'}, $J_{5'-6'} = 7.6$ Hz), 7.10 (d, 1H, H₈, $J_{6-8} = 1.6$ Hz), 6.92 (d, 1H, H₆, $J_{6-8} = 1.6$ Hz), 6.76 (d, 1H, H_{5'}, $J_{5'-6'} = 7.6$ Hz), 5.38 (d, 2H, H₂, $J_{\text{all}} = 2.0$ Hz), 3.07 (s, 6H, 2CH₃). ¹³C NMR (CDCl₃, 100 MHz): δ (ppm) 179.24, 162.65, 151.19, 139.39, 139.17, 135.92, 132.59, 126.01,

125.43, 123.38, 122.48, 119.29, 117.17, 112.13, 68.46, 40.29. Anal. Calcd. for C₁₇H₁₄Cl₂N₂O₂: C, 58.47; H, 4.04; Cl, 20.30; N, 8.02. Found: C, 58.28; H, 3.95; Cl, 20.35; N, 8.09.

4.1.2.11. (*E*)-3-[(1*H*-Indol-3-yl)methylene]chroman-4-one (**Ik**). Yield: 38%, mp = 221-222 °C. IR (KBr): 3241, 1643 cm⁻¹. ¹H NMR (DMSO-d₆, 400 MHz): δ (ppm) 12.10 (bs, 1H, NH), 8.09 (s, 1H, =CH), 7.91 (d, 1H, H₅, *J*₅₋₆ = 8.0 Hz), 7.82 (d, 1H, H_{7'}, *J*_{6'-7'} = 7.6 Hz), 7.80 (s, 1H, H_{2'}), 7.56 (t, 1H, H₇, *J*₇₋₈ = *J*₇₋₆ = 8.0 Hz), 7.51 (d, 1H, H_{4'}, *J*_{4'-5'} = 7.6 Hz), 7.26 (t, 1H, H_{6'}, *J*_{6'-7'} = *J*_{5'-6'} = 7.6 Hz), 7.20 (t, 1H, H_{5'}, *J*_{5'-6'} = *J*_{4'-5'} = 7.6 Hz), 7.12 (t, 1H, H₆, *J*₅₋₆ = *J*₇₋₆ = 8.0 Hz), 7.06 (d, 1H, H₈, *J*₇₋₈ = 8.0 Hz), 5.49 (s, 2H, H₂). ¹³C NMR (DMSO-d₆, 100 MHz): δ (ppm) 180.03, 160.32, 136.11, 135.38, 129.53, 127.63, 127.50, 126.98, 124.23, 122.75, 121.76, 121.57, 120.80, 118.19, 117.63, 112.20, 110.36, 68.55. Anal. Calcd. for C₁₈H₁₃N₂O₂: C, 78.53; H, 4.76; N, 5.09. Found: C, 78.73; H, 4.71; N, 5.13.

4.1.2.12. (*E*)-3-[(1*H*-Pyrrol-2-yl)methylene]chroman-4-one (**Il**). Yield: 64%, mp = 203-204 °C. IR (KBr): 3276, 1649 cm⁻¹. ¹H NMR (DMSO-d₆, 400 MHz): δ (ppm) 11.71 (bs, 1H, NH), 7.91 (d, 1H, H₅, *J*₅₋₆ = 8.0 Hz), 7.69 (s, 1H, =CH), 7.56 (t, 1H, H₇, *J*₇₋₈ = *J*₇₋₆ = 8.0 Hz), 7.21 (s, 1H, H_{3'}), 7.10 (t, 1H, H₆, *J*₅₋₆ = *J*₇₋₆ = 8.0 Hz), 7.04 (d, 1H, H₈, *J*₇₋₈ = 8.0 Hz), 6.57 (s, 1H, H_{5'}), 6.35 (s, 1H, H_{4'}), 5.41 (s, 2H, H₂). ¹³C NMR (DMSO-d₆, 100 MHz): δ (ppm) 179.86, 160.27, 135.35, 127.25, 126.88, 125.64, 124.09, 122.44, 121.63, 121.52, 117.59, 115.12, 111.58, 67.87. Anal. Calcd. for C₁₄H₁₁N₂O₂: C, 74.65; H, 4.92; N, 6.22. Found: C, 74.78; H, 4.97; N, 6.23.

4.1.2.13. (*E*)-3-[(1*H*-Imidazol-4-yl)methylene]chroman-4-one (**Im**). Yield: 78%, mp = 197-198 °C. IR (KBr): 3385, 1667 cm⁻¹. ¹H NMR (DMSO-d₆, 400 MHz): δ (ppm) 12.49 (bs, 1H, NH), 7.93 (s, 1H, =CH), 7.88 (dd, 1H, H₅, *J*₅₋₆ = 8.0 Hz, *J*₅₋₇ = 1.6 Hz), 7.80 (s, 1H, H_{3'}), 7.58-7.54 (m, 2H, H₇, H_{5'}), 7.11 (t, 1H, H₆, *J*₅₋₆ = *J*₇₋₆ = 8.0 Hz), 7.06 (d, 1H, H₈, *J*₇₋₈ = 8.4 Hz), 5.85 (d, 2H, H₂, *J*_{all} = 0.8 Hz). ¹³C NMR (DMSO-d₆, 100 MHz): δ (ppm) 181.18, 160.99, 137.86, 136.23, 135.48, 127.33, 127.10, 125.31,

125.06, 121.87, 121.49, 117.76, 67.73. Anal. Calcd. for C₁₃H₁₀N₂O₂: C, 69.02; H, 4.46; N, 12.38. Found: C, 69.21; H, 4.52; N, 12.33.

4.1.2.14. (*E*)-5,7-Dichloro-3-[(1*H*-imidazol-4-yl)methylene]chroman-4-one (**1n**) Yield: 23%, mp = 252-253 °C from n-hexane. IR (KBr): 3248, 1667 cm⁻¹. ¹H NMR (DMSO-d₆, 400 MHz): δ(ppm) 12.76 (bs, 1H, NH), 7.91 (s, 1H, =CH), 7.81 (s, 1H, H3'), 7.55 (s, 1H, H8), 7.30 (s, 1H, H6), 7.24 (s, 1H, H5'), 5.81 (s, 2H, H2). ¹³C NMR (DMSO-d₆, 100 MHz): δ(ppm) 192.25, 163.03, 138.33, 138.07, 136.29, 135.12, 135.73, 134.54, 125.11, 124.43, 118.84, 117.35, 68.07. Anal. Calcd. for C₁₃H₈Cl₂N₂O₂: C, 52.91; H, 2.73; Cl, 24.03; N, 9.49. Found: C, 53.08; H, 2.77; Cl, 24.11; N, 9.53.

4.1.2.15. (*E*)-3-[(1*H*-imidazol-4-yl)methylene]-7-methoxychroman-4-one (**1o**). Yield: 63%, mp = 176-178 °C from n-hexane. IR (KBr): 3112, 1679 cm⁻¹. ¹H NMR (DMSO-d₆, 400 MHz): δ(ppm) 12.59 (bs, 1H, NH), 7.90 (s, 1H, =CH), 7.79 (d, 1H, H5, *J*₅₋₆ = 8.4 Hz), 7.74 (s, 1H, H3'), 7.51 (s, 1H, H5'), 6.67 (dd, 1H, H6, *J*₅₋₆ = 8.4 Hz, *J*₆₋₈ = 2.0 Hz), 6.57 (d, 1H, H8, *J*₆₋₈ = 2.0 Hz), 5.82 (s, 2H, H2), 3.83 (s, 3H, OCH₃). ¹³C NMR (DMSO-d₆, 100 MHz): δ(ppm) 179.93, 165.18, 162.95, 137.65, 136.68, 128.82, 126.68, 125.32, 124.07, 115.47, 109.94, 100.83, 68.02, 55.68. Anal. Calcd. for C₁₄H₁₂N₂O₃: C, 65.62; H, 4.72; N, 10.93. Found: C, 65.78; H, 4.78; N, 10.88.

4.1.2.16. (*E*)-3-[(Furan-2-yl)methylene]chroman-4-one (**1p**). Yield: 87%, mp = 118-119 °C (lit. 105 °C [19]). IR (KBr): 1668 cm⁻¹. ¹H NMR (CDCl₃, 400 MHz): δ(ppm) 7.99 (d, 1H, H5, *J*₅₋₆ = 8.0 Hz) 7.59 (s, 1H, =CH), 7.50 (s, 1H, H3'), 7.45 (t, 1H, H7, *J*₇₋₈ = *J*₇₋₆ = 8.0 Hz), 7.03 (t, 1H, H6, *J*₅₋₆ = *J*₇₋₆ = 8.0 Hz), 6.96 (d, 1H, H8, *J*₇₋₈ = 8.0 Hz), 6.73 (s, 1H, H5'), 6.52 (s, 1H, H4'), 5.57 (s, 2H, H2). ¹³C NMR (CDCl₃, 100 MHz): δ(ppm) 181.53, 161.43, 151.37, 145.61, 135.59, 127.82, 126.80, 122.02, 121.75, 121.71, 118.50, 117.88, 112.66, 67.98. Anal. Calcd. for C₁₄H₁₀O₃: C, 74.33; H, 4.46. Found: C, 74.54; H, 4.47.

4.1.2.17. (*E*)-3-[(Thiophen-2-yl)methylene]chroman-4-one (**1q**). Yield: 85%, mp = 126-127 °C (lit. 125-126 °C) [16]. IR (KBr): 1661 cm⁻¹. ¹H NMR (CDCl₃, 400 MHz): δ (ppm) 8.01 (d, 1H, H5, $J_{5-6} = 7.2$ Hz), 7.98 (s, 1H, =CH), 7.59 (d, 1H, H3', $J_{3'-4'} = 4.4$ Hz), 7.48 (t, 1H, H7, $J_{7-8} = J_{7-6} = 7.2$ Hz), 7.34 (d, 1H, H5', $J_{4'-5'} = 4.4$ Hz), 7.16 (t, 1H, H4', $J_{3'-4'} = J_{4'-5'} = 4.4$ Hz), 7.06 (t, 1H, H6, $J_{5-6} = J_{7-6} = 7.2$ Hz), 6.98 (d, 1H, H8, $J_{7-8} = 7.2$ Hz), 5.46 (d, 2H, H2, $J_{\text{all}} = 1.2$ Hz). ¹³C NMR (CDCl₃, 100 MHz): δ (ppm) 181.24, 161.02, 137.67, 135.69, 133.88, 130.94, 128.70, 128.20, 127.87, 127.28, 121.95, 121.89, 117.83, 67.81. Anal. Calcd. for C₁₄H₁₀O₂S: C, 69.40; H, 4.16; S, 13.23. Found: C, 69.26; H, 4.16; S, 13.28.

4.1.2.18. (*E*)-3[-(Thiophen-3-yl)methylene]chroman-4-one (**1r**). Yield: 14%, mp = 105-106 °C. IR (KBr): 1664 cm⁻¹. ¹H NMR (CDCl₃, 400 MHz): δ (ppm) 7.98 (d, 1H, H5, $J_{5-6} = 7.2$ Hz), 7.78 (s, 1H, =CH), 7.44 (t, 1H, H7, $J_{7-8} = J_{7-6} = 7.2$ Hz), 7.37-7.36 (m, 2H, H2', H4'), 7.13 (d, 1H, H5', $J_{4'-5'} = 3.2$ Hz), 7.02 (t, 1H, H6, $J_{5-6} = J_{7-6} = 7.2$ Hz), 6.93 (d, 1H, H8, $J_{7-8} = 7.2$ Hz), 5.35 (d, 2H, H2, $J_{\text{all}} = 0.8$ Hz). ¹³C NMR (CDCl₃, 100 MHz): δ (ppm) 181.67, 161.03, 136.02, 135.72, 130.26, 129.22, 129.04, 128.84, 127.86, 126.69, 121.99, 121.85, 117.87, 67.88. Anal. Calcd. for C₁₄H₁₀O₂S: C, 69.40; H, 4.16; S, 13.23. Found: C, 69.31; H, 4.14; S, 13.20.

4.2. Biochemistry

4.2.1. Determination of hMAO Isoform Activity

The potential effects of the tested compounds on hMAO activity were investigated by measuring their effects on the production of hydrogen peroxide (H₂O₂) from *p*-tyramine, using the Amplex Red MAO assay kit (Molecular Probes, Inc., Eugene, Oregon, USA) and microsomal MAO isoforms prepared from insect cells (BTI-TN-5B1-4) infected with recombinant baculovirus containing cDNA inserts for hMAO-A or hMAO-B (Sigma-Aldrich Química S.A., Alcobendas, Spain). In this study hMAO activity was evaluated using the above method following the general procedure previously

described by us [21]. A brief description of the procedure is provided in Supplementary data. The tested drugs (new compounds and reference inhibitors) themselves were unable to react directly with the Amplex Red reagent, which indicates that these compounds do not interfere with the measurements.

4.2.2. Reversibility and Irreversibility Assays

To evaluate whether **1c** is a reversible or irreversible hMAO-B inhibitor, a dilution method was used [22]. A 100X concentration of the enzyme used in the above described experiments was incubated with a concentration of inhibitor equivalent to 10-fold its IC_{50} . After 30 min, the mixture was diluted 100-fold into reaction buffer containing Amplex® Red reagent, horseradish peroxidase and *p*-tyramine and reaction was monitored for 15 minutes. Reversible inhibitors show a linear progress with a slope equal to about 91% of the slope of the control sample while irreversible inhibition reaches only about 9% of this slope. Control tests were carried out by pre-incubating and diluting in the absence of inhibitor.

4.3. Molecular Modeling.

Protein Data Bank (PDB) [25] crystallographic structures 2Z5X [26] and 2V5Z [27] were considered for building our theoretical models of hMAO-A and hMAO-B respectively. In order to be suitable in docking simulation, the original PDB entries required preliminary manipulations, following the same approach of a previously reported manuscript [28]. The co-crystallised reversible ligands, harmine for 2Z5X and safinamide for 2V5Z, and water molecules were removed. FAD cofactor bonds order was fixed and hydrogen atoms were added to final models. In order to allow an optimal positioning of the hydrogen atoms, modified structures were submitted to protein heavy atoms constrained energy minimisation using 10,000 steps of the Polak Ribiere Conjugate Gradient algorithm as implemented in MacroModel program [29]. The constant force applied to not hydrogen atoms was equal to 50 kJ/mol·Å.

Optimised structures were considered as targets models of hMAO-A and hMAO-B and, in both cases, the ligand binding site was considered as a regular box of 27,000 Å³ centred onto the N5 FAD atom.

The theoretical structure of all our inhibitors was built by means of the Maestro GUI [30].

Glide software [31] was considered for docking simulation using the standard precision (SP) search algorithms. The ligands possible conformations were taken into account by the Glide flexible docking implementation. Default software scoring function (GScore) was applied for ranking docking poses.

The hMAO-A and hMAO-B models, both including the docking top ranked **1c** pose and ligand free, were explicitly solvated with water molecules included by the “Soak” method as implemented in Impact [32]. For all structures a regular box, of 64,000 Å³ centred onto the N5 FAD atom, was considered for the preliminary water positioning. Finally, after default refinement, 244/326 and 289/304 solvent molecules were retrieved in hMAO-A and hMAO-B complexes/ligand free respectively.

The resulting models were considered as starting structures for explicit solvent Molecular Dynamics (MD) simulation carried out using the Desmond software [33]. The SPC method was applied for generating solvated systems suitable for MD. The overall electrostatic net charge of the starting structures was neutralized including 3 Cl⁻ ions into the hMAO-A models and 3 Na⁺ ions into the hMAO-B ones. According to Desmond default protocol, solvated systems were equilibrated by means of 7 short and low temperature runs followed by the production simulation carried out at 300 °K, up to 1.2 ns, using an integration time step equal to 2 fs. The output MD trajectories consisted in 120 structures sampled at regular time intervals equal to 10 ps.

Ligand target interactions were computed by means of Maestro GUI.

Appendix A. Supplementary data

Supplementary data related to this article can be found at ...

References

- [1] A.S. Kalgutkar, D.K. Dalvie, N. Castagnoli, T.J. Taylor, Interactions of nitrogen-containing xenobiotics with monoamine oxidase (MAO) isozymes A and B: SAR studies on MAO substrates and inhibitors. *Chem. Res. Toxicol.* 14 (2001) 1139-1162.
- [2] M. Yamada, H. Yasuhara, Clinical pharmacology of MAO inhibitors: safety and future, *Neurotoxicol.* 25 (2004) 215-221.
- [3] M.C. Carreiras, J.L. Marco, Recent approaches to novel anti-Alzheimer's therapy, *Curr. Pharm. Des.* 10 (2004) 3167-3175.
- [4] H.H. Fernandez, J.J. Chen, Monoamine oxidase-B inhibition in the Parkinson's disease, *Pharmacother.* 27 (2007) 174S-185S.
- [5] F. Chimenti, R. Fioravanti, A. Bolasco, P. Chimenti, D. Secci, F. Rossi, M. Yañez, F. Orallo, F. Ortuso, S. Alcaro, Chalcones: A valid scaffold for Monoamine Oxidases inhibitors, *J. Med. Chem.* 52 (2009) 2818-2824.
- [6] F. Chimenti, R. Fioravanti, A. Bolasco, P. Chimenti, D. Secci, F. Rossi, M. Yanez, F. Orallo, F. Ortuso, S. Alcaro, A new series of flavones, thioflavones, and flavanones as selective monoamine oxidase-B inhibitors, *Bioorg. Med. Chem.* 18 (2010) 1273-1279.
- [7] N. Desideri, A. Bolasco, R. Fioravanti, L. Proietti Monaco, F. Orallo, M. Yañez, F. Ortuso, S. Alcaro, Homoisoflavonoids: Natural scaffold with Potent and Selective Monoamine Oxidase-B Inhibition Properties, *J. Med. Chem.* 54 (2011) 2155-2164.
- [8] N. Desideri, R. Fioravanti, L. Proietti Monaco, M. Biava, M. Yañez, F. Ortuso, S. Alcaro, 1,5-Diphenylpenta-2,4-dien-1-ones as potent and selective monoamine oxidase-B inhibitors, *Eur. J. Med. Chem.* 59 (2013) 91-100.
- [9] S.J. Robinson, J.P. Petzer, A. Petzer, J.J. Bergh, A.C.U. Lourens, Selected furanochalcones as inhibitors of monoamine oxidase, *Bioorg. Med. Chem. Lett.* 23 (2013) 4985-4989.

- [10] G. Jo, S. Ahn, B.G. Kim, H.R. Park, Y.H. Kim, H.A. Choo, D. Koh, Y. Chong, J.H. Ahn, Y. Lim, Chromenylchalcones with inhibitory effects on monoamine oxidase-B, *Bioorg. Med. Chem.* 21 (2013) 7890-7897.
- [11] A. Lévai, Synthesis of exocyclic α,β -unsaturated ketones, *ARKIVOC* (2004) (vii) 15-33.
- [12] P. Bennett, J.A. Donnelly, D.C. Meaney, P. O'Boyle, Stereochemistry of cyclopropyl ketones from the reaction of dimethylsulphoxonium methylide with 3-benzylidenechroman-4-ones, *J. Chem. Soc., Perkin Trans.1* (1972) 1554-1959.
- [13] A. Lévai, C. Nemes, T. Patonay, Synthesis of new (*Z*)-3-arylidenechromanones by the photoisomerization of (*E*)-3-arylidenechromanones, *Heterocycl. Commun.* 5 (1999) 441-444.
- [14] V. Siddaiah, C.V. Rao, S. Venkateswarlu, A.V. Krishnaraju, G.V. Subbaraju, Synthesis, stereochemical assignments, and biological activities of homoisoflavonoids, *Bioorg. Med. Chem.* 14 (2006) 2545-2551.
- [15] B. Kupcewicz, G. Balcerowska-Czerniak, M. Małecka, P. Paneth, U. Krajewska, M. Rozalski, Structure–cytotoxic activity relationship of 3-arylidene flavanone and chromanone (*E,Z* isomers) and 3-arylflavones, *Bioorg. Med. Chem. Lett.* 23 (2013) 4102–4106.
- [16] A. Levai, Z. Szabo, Synthesis of exocyclic α,β -unsaturated ketones, *Pharmazie*, 47 (1992) 56-57.
- [17] F. Fournier, J. Berthelot, A.M. Pavard, Anticholinesterase compounds. Structure-activity relationships of carbamates and phosphates, *Eur. J. Med. Chem.* 16 (1981) 48-58.
- [18] U. Thapa, P. Thapa, R. Karki, M. Yun, J.H. Choi, Y. Jahng, E. Lee, K.H. Jeon, Y. Na, E.M. Ha, W.J. Cho, Y. Kwon, E.S. Lee, Synthesis of 2,4-diaryl chromenopyridines and evaluation of their topoisomerase I and II inhibitory activity, cytotoxicity, and structure-activity relationship, *Eur. J. Med. Chem.* 46 (2011) 3201-3209.
- [19] K. M. Tapas, P. Rammohan, M. Rina, K.M. Asok, Facile condensation of aromatic aldehydes with chroman-4-ones and 1-thiochroman-4-ones catalysed by Amberlyst-15 under microwave irradiation condition, *E-J. Chem.* 8(2) (2011) 863-869.

- [20] B.L. Zhao, D.M. Du, Chiral Squaramide-Catalyzed Michael/Alkylation Cascade Reaction for the Asymmetric Synthesis of Nitro-Spirocyclopropanes, *Eur. J. Org. Chem.* 24 (2015) 5350-5359.
- [21] M. Yáñez, N. Fraiz, E. Cano, F. Orallo, Inhibitory effects of cis- and trans-resveratrol on noradrenalina and 5-hydroxytryptamine uptake and on monoamine oxidase activity, *Biochem. Biophys. Res. Commun.* 344 (2006) 688-695.
- [22] R.A. Copeland, *Evaluation of Enzyme Inhibitors in Drug Discovery*, Wiley Interscience, Hoboken, 2005.
- [23] L. Basile, M. Pappalardo, S. Guccione, D. Milardi, R.R. Ramsay, Computational comparison of imidazoline association with the I2 binding site in human monoamine oxidases. *J. Chem. Inf. Model.* 54 (2014) 1200–1207.
- [24] J. Juárez-Jiménez, E. Mendes, C. Galdeano, C. Martins, D.B. Silva, J. Marco-Contelles, M. do Carmo Carreiras, F.J. Luque, R.R. Ramsay, Exploring the structural basis of the selective inhibition of monoamine oxidase A by dicyanitrile aminoheterocycles: role of Asn181 and Ile335 validated by spectroscopic and computational studies. *Biochim. Biophys. Acta.* 1844 (2014) 389-397.
- [25] H.M. Berman, J. Westbrook, Z. Feng, G. Gilliland, T.N. Bhat, H. Weissig, I.N. Shindyalov, P.E. Bourne, The Protein Data Bank, *Nucleic Acids Res.* 28 (2000) 235-242.
- [26] S.Y. Son, J. Ma, Y. Kondou, M. Yoshimura, E. Yamashita, T. Tsukihara, Structure of human monoamine oxidase A at 2.2 Å resolution: the control of opening the entry for substrates/inhibitors, *Proc. Natl. Acad. Sci. USA.* 15 (2008) 5739-5744.
- [27] C. Binda, J. Wang, L. Pisani, C. Caccia, A. Carotti, P. Salvati, D.E. Edmondson, A. Mattevi, Structures of human monoamine oxidase B complexes with selective noncovalent inhibitors: safinamide and coumarin analogs, *J. Med. Chem.* 23 (2007) 5848-5852.
- [28] F. Chimenti, A. Bolasco, D. Secci, P. Chimenti, A. Granese, S. Carradori, M. Yanez, F. Orallo, F. Ortuso, S. Alcaro, Investigations on the 2-thiazolyldrazine scaffold: synthesis and molecular modeling of selective human monoamine oxidase inhibitors, *Bioorg. Med. Chem.* 18 (2010) 5715-5723.

- [29] MacroModel, version 10.8, Schrödinger, LLC, New York, NY, 2015.
- [30] Maestro, version 10.2, Schrödinger, LLC, New York, NY, 2015.
- [31] Glide, version 6.7, Schrödinger, LLC, New York, NY, 2015.
- [32] Impact version 6.7, Schrödinger, LLC, New York, NY, 2015.
- [33] Desmond Molecular Dynamics System, version 4.2, D. E. Shaw Research, New York, NY, 2015.

- A series of (*E*)-3-heteroarylidenochroman-4-ones was synthesized.
- The compounds were evaluated *in vitro* as inhibitors of both human MAO isoforms.
- All the compounds were found to be selective hMAO-B inhibitors.
- The most active compound showed MAO-B inhibitory activity in the nanomolar range.
- Docking and molecular dynamics simulations proposed the binding mode of the best compound.

ACCEPTED MANUSCRIPT